FLUID DYNAMICS

Numerical Investigation of Natural Convection and Entropy Generation in a Square Enclosure Filled with Cu-Fe_3O_4/Water Hybrid Nanofluid under the Impact of Discrete Heat Sources

S. Gowtham

Department of Mathematics, Karpagam Academy of Higher Education, Coimbatore, Tamil Nadu, India

Published November 2026

Abstract

This study investigates magnetohydrodynamic (MHD) natural convection and total entropy generation of a Cu-Fe_3O_4/water hybrid nanofluid in a two-dimensional square enclosure equipped with a discrete bottom heat source. The left and right vertical walls are maintained at a cold temperature T_c, the top horizontal boundary is thermally insulated, and the bottom horizontal wall features a centrally positioned localized heat source kept at a high temperature T_h. The non-dimensional governing conservation equations—mass, momentum, and thermal energy—are solved numerically using the Finite Volume Method (FVM) coupled with the SIMPLE algorithm. The investigation evaluates a parametric domain: Rayleigh number ($10^3 \le Ra \le 10^6$), Hartmann number ($0 \le Ha \le 60$), solid volume fraction of hybrid nanoparticles ($0 \le \varphi \le 0.04$), and heat source length ($0.2 \le \varepsilon \le 0.8$). Results show that increasing the Rayleigh number and expanding the heat source length enhance natural convection strength, local/average Nusselt numbers (Nu), and total entropy generation. Conversely, applying a magnetic field ($Ha > 0$) induces opposing Lorentz forces that suppress fluid circulation, dampening convective heat transfer and overall irreversibility. The addition of Cu-Fe_3O_4 hybrid nanoparticles yields superior heat transfer rates compared to single-nanoparticle suspensions and pure water. Bejan number (Be) analysis demonstrates a transition from thermal-irreversibility domination at low Ha to viscous and magnetic irreversibility domination at higher magnetic field strengths.

Keywords: Natural convection; entropy generation; Cu-Fe_3O_4 hybrid nanofluid; discrete heat source; magnetohydrodynamics (MHD); finite volume method; Bejan number

1 Introduction

Convective heat transfer driven by localized heat sources within enclosed cavities is relevant to modern thermal management applications, including electronic component cooling, micro-channel heat sinks, solar energy receivers, transformer oil cooling, and nuclear safety systems. In these configurations, non-uniform thermal boundary conditions generate complex buoyant flow structures, requiring detailed numerical analysis for optimal design. To overcome the low thermal conductivity of standard thermal transport fluids (such as water, ethylene glycol, and engine oil), suspensions of nanoscale metallic or metal-oxide particles—termed nanofluids—have been extensively studied. Recent advances focus on hybrid nanofluids, which combine two distinct nanoparticle species to leverage synergistic chemical, magnetic, and thermal features. Combining metallic Copper (Cu)—known for its high thermal conductivity—with Magnetite (Fe_3O_4)—a ferrofluid component with strong magnetic responsiveness—yields a hybrid fluid (Cu-Fe_3O_4/water) suitable for active flow control and heat transfer enhancement.

Applying external magnetic fields introduces electromagnetic forces (Lorentz forces) that damp buoyant circulation patterns, allowing active thermal flow regulation. In addition to First-Law thermal performance, Second-Law thermodynamic optimization (minimizing entropy generation) is critical for design efficiency.

This work provides a systematic numerical evaluation of natural convection, heat transfer enhancement, total entropy generation, and Bejan number behavior for a Cu-Fe_3O_4/water hybrid nanofluid contained in a square cabinet with a discrete bottom heat source under a magnetic field.

2 Physical model and mathematical formulation

2.1 Geometric configuration

Figure 1 shows the physical model of the problem.

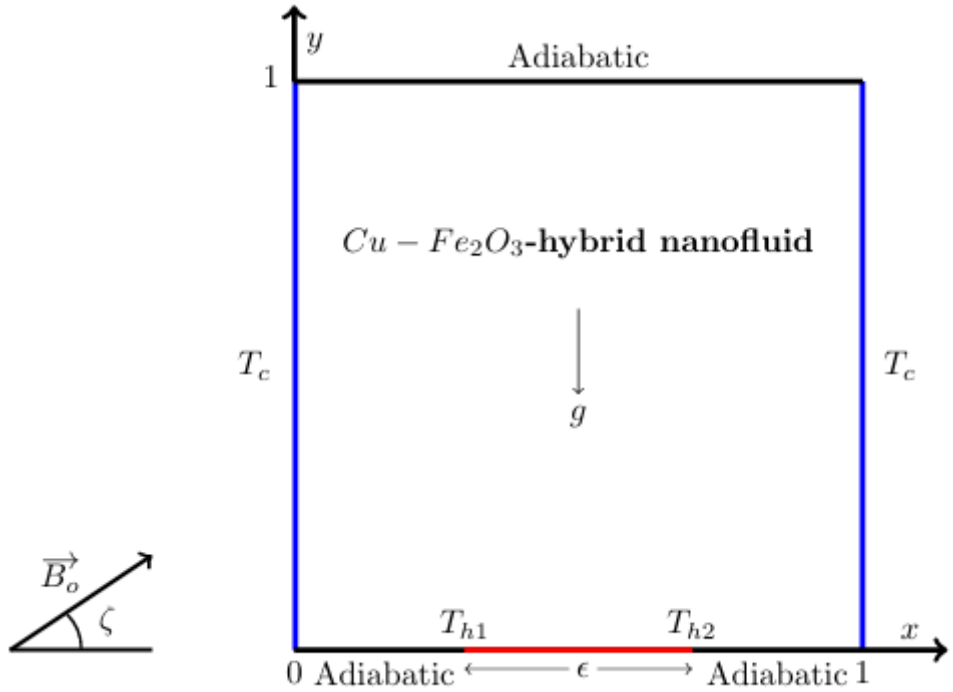


Figure 1. Physical model of the problem.

Consider a two-dimensional square enclosure of height and width L. A discrete heat source of length $w = \varepsilon L$ ($0.2 \le \varepsilon \le 0.8$) is located at the center of the bottom horizontal wall at temperature T_h. The remaining parts of the bottom wall and the entire top wall are thermally insulated ($\partial T/\partial y = 0$). The left and right vertical walls are maintained at a constant cold temperature T_c ($T_h > T_c$). The cavity is filled with an incompressible, Newtonian Cu-Fe_3O_4/water hybrid nanofluid. A uniform magnetic field $B = B_0 \hat{i}$ is applied horizontally. The thermophysical properties of water, Fe_3O_4, and Cu are presented in Table 1.

Table 1. Thermophysical properties of water and nanoparticles at T = 300 K.

Property	Base Fluid (H_2O)	Fe_3O_4 (Magnetite)	Cu (Copper)
Density ρ (kg/m^3)	997.1	5180	8933

Property	Base Fluid (H_2O)	Fe_3O_4 (Magnetite)	Cu (Copper)
Specific Heat Cp (J/kg·K)	4179	670	385
Thermal Conductivity k (W/m·K)	0.613	9.7	400
Electrical Conductivity σ ($\Omega^{-1}m^{-1}$)	0.05	25000	5.96×10^7
Thermal Expansion β (K^{-1})	2.1×10^{-4}	1.3×10^{-5}	1.67×10^{-5}

2.2 Governing equations

Assuming steady, laminar, two-dimensional, incompressible flow with Boussinesq approximations for density variations, the dimensional conservation equations are:

$$\frac{\partial u}{\partial x} + \frac{\partial v}{\partial y} = 0 \tag{1}$$

$$u\frac{\partial u}{\partial x} + v\frac{\partial u}{\partial y} = -\frac{1}{\rho_{hnf}}\frac{\partial p}{\partial x} + \nu_{hnf}\left(\frac{\partial^2 u}{\partial x^2} + \frac{\partial^2 u}{\partial y^2}\right) \tag{2}$$

$$u\frac{\partial v}{\partial x} + v\frac{\partial v}{\partial y} = -\frac{1}{\rho_{hnf}}\frac{\partial p}{\partial y} + \nu_{hnf}\left(\frac{\partial^2 v}{\partial x^2} + \frac{\partial^2 v}{\partial y^2}\right) + \frac{(\rho\beta)_{hnf}}{\rho_{hnf}}g(T - T_c) - \frac{\sigma_{hnf}B_0^2}{\rho_{hnf}}v \tag{3}$$

$$u\frac{\partial T}{\partial x} + v\frac{\partial T}{\partial y} = \alpha_{hnf}\left(\frac{\partial^2 T}{\partial x^2} + \frac{\partial^2 T}{\partial y^2}\right) \tag{4}$$

2.3 Non-dimensionalization

Using non-dimensional variables:

$$X = \frac{x}{L},\ Y = \frac{y}{L},\ U = \frac{uL}{\alpha_f},\ V = \frac{vL}{\alpha_f},\ P = \frac{pL^2}{\rho_f\alpha_f^2},\ \Theta = \frac{T - T_c}{T_h - T_c} \tag{5}$$

The non-dimensional governing equations are:

$$\frac{\partial U}{\partial X} + \frac{\partial V}{\partial Y} = 0 \tag{6}$$

$$U\frac{\partial U}{\partial X} + V\frac{\partial U}{\partial Y} = -\frac{\partial P}{\partial X} + \Pr\frac{\rho_f}{\rho_{hnf}}\frac{1}{(1-\varphi)^{2.5}}\left(\frac{\partial^2 U}{\partial X^2} + \frac{\partial^2 U}{\partial Y^2}\right) \tag{7}$$

$$U\frac{\partial V}{\partial X} + V\frac{\partial V}{\partial Y} = -\frac{\partial P}{\partial Y} + \Pr\frac{\rho_f}{\rho_{hnf}}\frac{1}{(1-\varphi)^{2.5}}\left(\frac{\partial^2 V}{\partial X^2} + \frac{\partial^2 V}{\partial Y^2}\right) + Ra\Pr\frac{(\rho\beta)_{hnf}}{\rho_f\beta_f}\Theta - Ha^2\Pr\frac{\sigma_{hnf}\rho_f}{\sigma_f\rho_{hnf}}V \tag{8}$$

$$U\frac{\partial \Theta}{\partial X} + V\frac{\partial \Theta}{\partial Y} = \frac{\alpha_{hnf}}{\alpha_f}\left(\frac{\partial^2 \Theta}{\partial X^2} + \frac{\partial^2 \Theta}{\partial Y^2}\right) \tag{9}$$

The key non-dimensional parameters are the Rayleigh number (Ra), the Prandtl number (Pr), the Hartmann number (Ha) and the dimensionless heat source ratio (ε):

$$Ra = \frac{g\beta_f(T_h - T_c)L^3}{\nu_f\alpha_f},\ \Pr = \frac{\nu_f}{\alpha_f},\ Ha = B_0L\sqrt{\frac{\sigma_f}{\mu_f}},\ \varepsilon = \frac{w}{L} \tag{10}$$

2.4 Thermophysical properties of the Cu-Fe_3O_4 hybrid nanofluid

Equal volume proportions of Fe_3O_4 (φ_1) and Cu (φ_2) nanoparticles are assumed ($\varphi_1 = \varphi_2 = \varphi/2$):

Density:

$$\rho_{hnf} = (1-\varphi)\rho_f + \varphi_1\rho_{p1} + \varphi_2\rho_{p2} \tag{11}$$

Heat capacity:

$$(\rho C_p)_{hnf} = (1-\varphi)(\rho C_p)_f + \varphi_1(\rho C_p)_{p1} + \varphi_2(\rho C_p)_{p2} \tag{12}$$

Thermal expansion coefficient:

$$(\rho\beta)_{hnf} = (1-\varphi)(\rho\beta)_f + \varphi_1(\rho\beta)_{p1} + \varphi_2(\rho\beta)_{p2} \tag{13}$$

Dynamic viscosity (Brinkman model [1]):

$$\mu_{hnf} = \frac{\mu_f}{(1-\varphi)^{2.5}} \tag{14}$$

Thermal conductivity (extended Maxwell model [2]):

$$\frac{k_{hnf}}{k_f} = \frac{\frac{\varphi_1 k_{p1} + \varphi_2 k_{p2}}{\varphi} + 2k_f + 2\left(\varphi_1 k_{p1} + \varphi_2 k_{p2}\right) - 2\varphi k_f}{\frac{\varphi_1 k_{p1} + \varphi_2 k_{p2}}{\varphi} + 2k_f - \left(\varphi_1 k_{p1} + \varphi_2 k_{p2}\right) + \varphi k_f} \tag{15}$$

Electrical conductivity (Maxwell model [2]):

$$\frac{\sigma_{hnf}}{\sigma_f} = 1 + \frac{3\left(\frac{\varphi_1\sigma_{p1} + \varphi_2\sigma_{p2}}{\sigma_f} - \varphi\right)}{\left(\frac{\varphi_1\sigma_{p1} + \varphi_2\sigma_{p2}}{\varphi\sigma_f} + 2\right) - \left(\frac{\varphi_1\sigma_{p1} + \varphi_2\sigma_{p2}}{\sigma_f} - \varphi\right)} \tag{16}$$

2.5 Entropy generation formulation

The local volumetric entropy generation rate (S_gen''') consists of thermal heat transfer (S_gen,th'''), fluid friction (S_gen,ff'''), and magnetic field (S_gen,mag''') irreversibilities:

$$S'''_{gen} = S'''_{gen,th} + S'''_{gen,ff} + S'''_{gen,mag} \tag{17}$$

$$S'''_{gen,th} = \frac{k_{hnf}}{T_0^2}\left[\left(\frac{\partial T}{\partial x}\right)^2 + \left(\frac{\partial T}{\partial y}\right)^2\right] \tag{18}$$

$$S'''_{gen,ff} = \frac{\mu_{hnf}}{T_0}\left[2\left(\frac{\partial u}{\partial x}\right)^2 + 2\left(\frac{\partial v}{\partial y}\right)^2 + \left(\frac{\partial u}{\partial y} + \frac{\partial v}{\partial x}\right)^2\right] \tag{19}$$

$$S'''_{gen,mag} = \frac{\sigma_{hnf}B_0^2 v^2}{T_0} \tag{20}$$

Integrating across the enclosure volume yields total dimensionless entropy generation (S_tot):

$$S_{tot} = \int_0^1\int_0^1 \left(S_{th} + S_{ff} + S_{mag}\right)dXdY \tag{21}$$

The Bejan number (Be) is defined as:

$$Be = \frac{S_{th}}{S_{tot}} = \frac{S_{th}}{S_{th} + S_{ff} + S_{mag}} \tag{22}$$

3 Numerical methodology and validation

3.1 Numerical scheme

The governing partial differential equations are discretized using the Finite Volume Method (FVM) on a non-uniform staggered grid. Convective terms are evaluated using a high-resolution power-law scheme, while diffusion terms use central differencing. The pressure-velocity coupling is handled via the SIMPLE algorithm. Iterative convergence is achieved when maximum residuals satisfy $\sum|\Phi_{ij}^{n+1} - \Phi_{ij}^{n}| \leq 10^{-7}$ for all variables.

3.2 Grid independence test

Grid refinement tests were conducted at Ra = 10^5, Ha = 30, φ = 0.02, and ε = 0.4 across five grid densities (40×40 to 120×120). Based on the average Nusselt number (Nu) convergence shown in Table 2, an 80×80 non-uniform grid clustered near boundaries and heat source edges was selected.

Table 2. Grid independence study at Ra = 105, Ha = 30, φ = 0.02, ε = 0.4.

Grid Mesh	Average Nusselt Number (Nu)	Total Entropy Generation (S_tot)	Relative Change in Nu (%)
40 × 40	4.1120	15.120	-
60 × 60	4.1855	15.410	1.78%
80 × 80	4.2081	15.535	0.54%
100 × 100	4.2120	15.550	0.09%
120 × 120	4.2131	15.555	0.02%

3.3 Code validation

The computational solver was validated against benchmark numerical data for a differentially heated square cavity filled with pure air (Pr = 0.71). Comparison with the benchmark solution of de Vahl Davis [3] shows agreement within < 0.3% relative error (Table 3).

Table 3. Code validation against the de Vahl Davis [3] benchmark data.

Rayleigh Number (Ra)	Present Study (Nu)	de Vahl Davis (Nu)	Absolute Deviation (%)
10^3	1.118	1.118	0.00%
10^4	2.245	2.243	0.09%
10^5	4.521	4.519	0.04%
10^6	8.825	8.800	0.28%

4 Results and discussion

4.1 Flow topology and isothermal profiles

Placing a discrete heat source along the bottom wall creates symmetrical counter-rotating flow cells. Fluid ascends above the central heated segment and descends along the cold vertical side walls.

Effect of Heat Source Length (ε): Expanding ε from 0.2 to 0.8 broadens the primary thermal plume, intensifying convective circulation and accelerating flow velocities.

Effect of Magnetic Field (Ha): Applying an external horizontal magnetic field (Ha > 0) induces a downward-acting Lorentz force opposing vertical fluid motion. At Ha = 60, circulation velocities decrease, the counter-rotating vortices shrink, and isotherms flatten into a conduction-like distribution.

4.2 Thermal performance and heat transfer analysis

Heat transfer from the discrete bottom heater is evaluated using the average Nusselt number across the heater length:

$$Nu = \frac{1}{\varepsilon}\int Nu_x dX \tag{23}$$

Table 4 presents the average Nusselt number (Nu) at varying Ra, Ha, φ and heat source length (ε).

Table 4. Average Nusselt number (Nu) at varying Ra, Ha, φ and heat source length (ε).

Ra	Ha	ε	Pure Water (ϕ = 0.00)	Cu-Fe_3O_4 (ϕ = 0.02)	Cu-Fe_3O_4 (ϕ = 0.04)
10^4	0	0.4	2.410	2.612	2.825
10^4	30	0.4	1.625	1.770	1.920
10^4	60	0.4	1.150	1.255	1.365
10^5	0	0.2	3.820	4.150	4.490
10^5	0	0.4	4.850	5.280	5.710
10^5	0	0.8	6.120	6.640	7.180
10^5	30	0.4	3.880	4.208	4.560
10^5	60	0.4	2.250	2.455	2.670
10^6	0	0.4	9.450	10.280	11.120
10^6	30	0.4	8.420	9.150	9.890
10^6	60	0.4	5.810	6.320	6.840

Key trends from Table 4 are as follows:

- Increasing nanoparticle volume fraction to φ = 0.04 yields a 17.7% enhancement in Nu relative to pure water at Ra = 10^5, ε = 0.4, Ha = 0.
- Increasing Hartmann number from Ha = 0 to Ha = 60 at Ra = 10^5 causes a ≈53.3% drop in Nu due to magnetic damping.
- Enlarging the heat source ratio from ε = 0.2 to ε = 0.8 increases total thermal energy dissipation, raising Nu by ≈60%.

4.3 Entropy generation and Bejan number analysis

Thermodynamic irreversibility components and average Bejan numbers (Be_avg) at Ra = 10^5 and ε = 0.4 are presented in Table 5.

Table 5. Entropy generation components and Bejan numbers at Ra = 105, ε = 0.4.

Hartmann No. (Ha)	Nanoparticle Fraction (ϕ)	S_th	S_ff	S_mag	S_tot	Average Bejan No. (Be)
0	0.00	9.12	3.45	0.00	12.57	0.725

Hartmann No. (Ha)	Nanoparticle Fraction (ϕ)	S_th	S_ff	S_mag	S_tot	Average Bejan No. (Be)
0	0.02	10.55	4.15	0.00	14.70	0.718
0	0.04	12.05	4.90	0.00	16.95	0.711
30	0.00	7.65	2.15	3.55	13.35	0.573
30	0.02	8.95	2.62	3.965	15.535	0.576
30	0.04	10.25	3.12	4.70	18.07	0.567
60	0.00	4.55	0.72	5.35	10.62	0.428
60	0.02	5.25	0.91	6.45	12.61	0.416
60	0.04	6.02	1.12	7.60	14.74	0.408

Key findings are as follows:

1. **Thermal Irreversibility (S_{th}):** Scales directly with nanoparticle concentration φ and heat source length ε due to elevated temperature gradients.
2. **Magnetic Irreversibility (S_{mag}):** Increases substantially at higher Hartmann numbers, dominating viscous losses at Ha = 60.
3. **Bejan Number (Be):** Decreases from ≈0.72 at Ha = 0 to ≈0.41 at Ha = 60, indicating a shift from heat-transfer-dominated to magnetic and viscous-dominated irreversibility.

5 Conclusions

This study modeled MHD natural convection, heat transfer enhancement, and total entropy generation for a Cu-Fe_3O_4/water hybrid nanofluid in a square cavity with a discrete bottom heat source. Key conclusions include:

Thermal Performance: Adding Cu-Fe_3O_4 hybrid nanoparticles to water increases average Nusselt numbers by up to 17.7% at φ = 0.04, outperforming pure water across all Rayleigh numbers.

Magnetic Suppression: Higher Hartmann numbers damp natural convection circulation cells via Lorentz forces. Increasing Ha from 0 to 60 decreases heat transfer by over 53% at Ra = 10^5.

Geometric Impact: Extending the heat source length ratio (ε) from 0.2 to 0.8 increases the overall Nusselt number by approximately 60%.

Second-Law Evaluation: Total entropy generation (S_tot) increases with nanoparticle volume fraction and heat source length. At high Hartmann numbers (Ha = 60), magnetic irreversibility dominates, reducing the Bejan number below 0.5.

These findings inform the thermodynamic optimization of localized thermal management systems utilizing hybrid magnetic nanofluids under external field control.

Table 6 presents the nomenclature.

Table 6. Nomenclature.

Symbol	Description	SI Units
B_0	External magnetic field strength	T
Be	Bejan number	-

Symbol	Description	SI Units
Cp	Specific heat capacity	J/(kg·K)
g	Gravitational acceleration	m/s^2
Ha	Hartmann number	-
k	Thermal conductivity	W/(m·K)
L	Side length of the square cabinet	m
Nu	Local Nusselt number	-
Nu_avg	Average Nusselt number	-
p, P	Dimensional and non-dimensional pressure	N/m^2, -
Pr	Prandtl number	-
Ra	Rayleigh number	-
S_gen'''	Volumetric entropy generation rate	$W/(m^3·K)$
S_tot	Total non-dimensional entropy generation rate	-
T	Temperature	K
u, v	Velocity components along x, y	m/s
U, V	Non-dimensional velocity components	-
w	Heat source physical length	m
x, y	Cartesian coordinates	m
X, Y	Non-dimensional coordinates	-

References

[1] Brinkman HC. The viscosity of concentrated suspensions and solutions. *The Journal of Chemical Physics*. 1952;20(4):571.

[2] Maxwell JC. *A treatise on electricity and magnetism*. Oxford: Clarendon Press; 1873.

[3] de Vahl Davis G. Natural convection of air in a square cavity: A bench mark numerical solution. *International Journal for Numerical Methods in Fluids*. 1983;3(3):249–264.

[4] Ghalambaz M, Hashem Zadeh SM, Veismoradi A, Sheremet MA, Pop I. Free convection heat transfer and entropy generation in an odd-shaped cavity filled with a Cu-Al2O3 hybrid nanofluid. *Symmetry*. 2021;13(1):122. https://doi.org/10.3390/sym13010122

[5] Tayebi T, Chamkha AJ. Entropy generation analysis during MHD natural convection flow of Cu-Al2O3/water hybrid nanofluid in a square cavity. *Entropy*. 2020;22(1):85.

[6] Kardgar A. Natural convection and entropy generation of non-Newtonian hybrid Cu-Al2O3/water nanofluid in an inclined partial porous cavity with different local heater positions in the presence of magnetic field. *Journal of Heat and Mass Transfer Research*. 2023;10(2):279–300. https://doi.org/10.22075/jhmtr.2023.30638.1442

[7] Selimefendigil F, Öztop HF. Effects of conductive curved partition and magnetic field on natural convection and entropy generation in an inclined cavity filled with nanofluid. *Physica A: Statistical Mechanics and its Applications*. 2020;540:123004.

[8] Aminossadati SM, Ghasemi B. Natural convection cooling of a localised heat source at the bottom of a nanofluid-filled enclosure. *European Journal of Mechanics - B/Fluids*. 2009;28(5):630–640.